Theory of Dielectric-Loaded and Tapered-Field Ferrite Devices*

R. F. SOOHOO†, SENIOR MEMBER, IRE

Summary—**Loading a ferrite resonance isolator or differential phase shifter with a dielectric or biasing the ferrite with an inhomogeneous dc magnetic field are very useful ways of improving the performance of these ferrite devices. Whereas these methods are very commonly used in transverse-field ferrite devices, no extensive analytical treatment of the subject has appeared in the literature. It is the purpose of this paper to present a theoretical analysis of the problem, chiefly by means of combined boundary-value and perturbation-theory approach. It will be shown that dielectric-loading and tapered-field techniques increase the bandwidth of isolators and phase shifters, the isolation-to-insertion loss ratio of the former, and the phase shift of the latter.**

Introduction

TWO of the most important contributions to the improvement of the characteristics of ferrite devices are 1) loading a ferrite resonance isolator or phase shifter with a dielectric, and 2) biasing the ferrite with an inhomogeneous dc magnetic field. Whereas these methods are in general use in present-day ferrite devices, the reasons for their remarkable success are not well understood. It is the purpose of this paper to investigate these problems analytically by means of a combined boundary-value and perturbation-theory approach. In the following sections, we will show that dielectric loading improves the ellipticity ratio and concentrates more energy in the ferrite over a large frequency band as compared with the unloaded case. We will also show that biasing the ferrite by a spatial varying dc magnetic field would give rise to a continuum rather than a single-resonance frequency, thereby increasing the bandwidth of the particular ferrite device.

Fig. 1(b) is the most common configuration used in dielectric-loaded ferrite devices. Because of the large number of boundaries at which the continuity of the tangential components of $\boldsymbol{E}$ and $\boldsymbol{h}$ must be satisfied, the exact solution of the problem is most difficult to obtain. The problem is further complicated by the fact that the ferrite and dielectric do not extend across the entire height of the waveguide, thus requiring the existence of other than the TE_{10} mode, even if the composite structure has such dimensions that all other modes are beyond cutoff. However, the problem is more amenable to treatment by the perturbation theory. In this case, we make the plausible assumption that the ferrite and dielectric cross sections are so small that the electromagnetic field outside the vicinity of the ferrite is not appreciably disturbed. For the configuration of Fig. 1(a), a more realistic solution to the problem may be obtained by solving a combined boundary-value and perturbation problem. Here, we first solve the exact boundary-value problem with only the dielectric slab present; then, the presence of the ferrite is treated as a perturbation.

Since the dc magnetic field is inhomogeneous in the ferrite in Fig. 1(c), the permeability of the ferrite is a function of x, thus rendering any exact boundary-value solution unfeasible. Furthermore, since $b \neq b'$, a pure TE_{10} mode can never exist. Here again, the perturbation theory could be advantageously used to get some physical insight into the behavior of this kind of device.

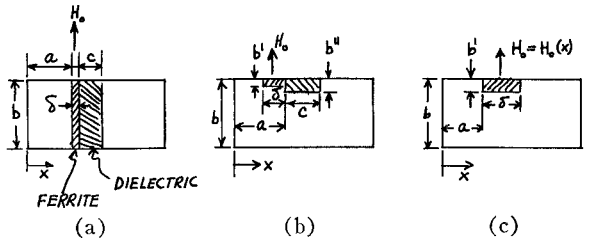

Fig. 1—Configuration of ferrite derives. (a) and (b) Dielectric-loaded devices. (c) Tapered-field devices.

Dielectric Loading

Consider first the case of Fig. 1(a) without the ferrite slab. If the dielectric is centrally located, we may plot $h_{x,y}(x)/\sqrt{P}$, where P is the waveguide power flow, by using the expressions given by Vartanian, *et al.*[1] as is done in Fig. 2 for $\epsilon_d = 9\epsilon_0$, and $kL = 5$ where $k = \omega\sqrt{\mu_0\epsilon_0}$ is the free-space wave number. For comparison, $h_{x,y}(x)$ for an empty waveguide is also shown. From Fig. 2, we note a drastic change in the RF magnetic field distribution due to the presence of the dielectric. In particular, we note that there is a high concentration of electromagnetic field near the dielectric where the ferrite is to be placed. Thus, other things being equal, the absorption and phase shift due to the presence of the ferrite should increase with dielectric loading.

* Received by the PGMTT, September 6, 1960; revised manuscript received, January 13, 1961. A brief account of some of the results of this paper was reported at the PGMTT Natl. Convention, Harvard University, Cambridge, Mass., June, 1959. The research for the paper was carried out while the author was with Cascade Res., Los Gatos, Calif.

† Lincoln Lab., Mass. Inst. Tech., Lexington, Mass.

[1] P. H. Vartanian, W. P. Ayres, and A. L. Helgesson, "Propagation in dielectric slab loaded rectangular waveguide," IRE TRANS. ON MICROWAVE THEORY AND TECHNIQUES, vol. MTT-6, pp. 215–222; April, 1958.

We note further that $h_x \simeq h_y$ over a large portion of the unfilled region of the guide. This result can best be illustrated by plotting h_{x1}/h_{y1} as is done in Fig. 3, again for a centrally-located slab. We note immediately that the ellipticity is remarkably close to unity over most of the unfilled portion of the guide. To emphasize this point, we have plotted in Fig. 3, also, the ellipticity in the same portion of an empty guide.

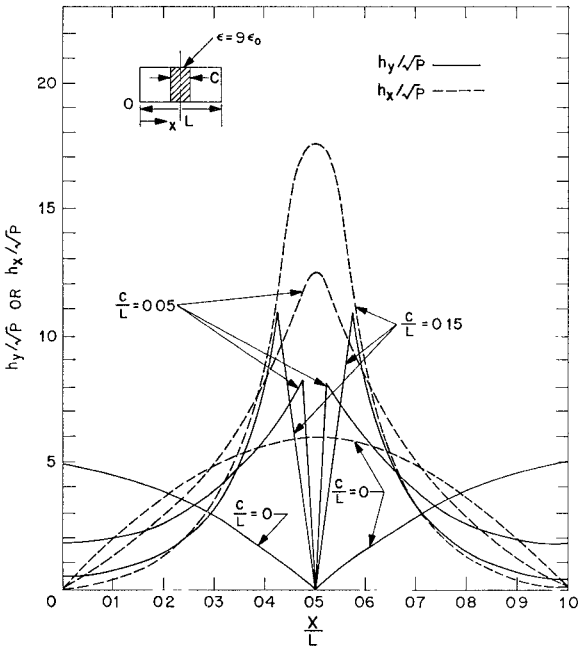

Fig. 2—Normalized RF magnetic-field component vs normalized distance from guidewall of a waveguide loaded by a centrally located dielectric slab at $kL=5$.

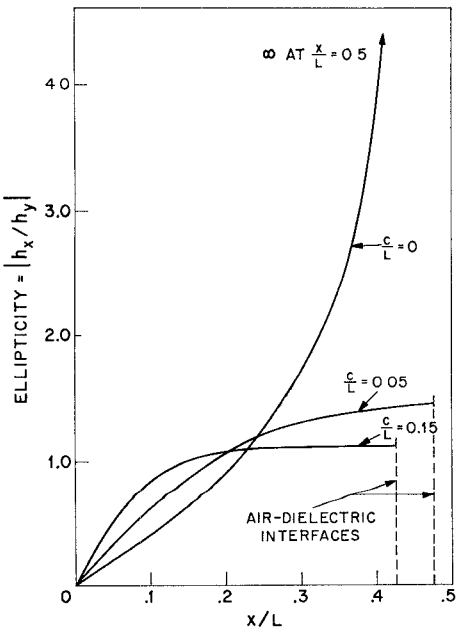

Fig. 3—Ellipticity vs normalized distance from guidewall of a waveguide loaded by a centrally-located dielectric slab at $kL=5$.

From the above discussion, we conclude that the most important effects of dielectric loading are:

1) *The concentration of the electromagnetic field in and near the dielectric*, and

2) *The two planes of circular polarization in an empty guide are smeared into two regions of near circular polarization.*

Next, we should like to investigate the dependence of ellipticity with frequency as is done in Fig. 4. For comparison, we have shown the ellipticity of the empty guide at a location x_0, so chosen that the ellipticity is equal to 1 at midband ($kL=5$). We note here that the variation of ellipticity with frequency may be greatly reduced by dielectric loading.[2]

Ferrite Perturbation

Now, if a thin ferrite slab is placed against the dielectric as shown in Fig. 1(a), a calculation of the propagation constant may be achieved by means of the perturbation formula:[3]

$$\gamma + \gamma_0^* = \frac{j\omega \int_{\Delta s} [(\Delta \mathfrak{y} \cdot \boldsymbol{H}) \cdot \boldsymbol{H}_0^* + (\Delta \epsilon \boldsymbol{E}) \cdot \boldsymbol{E}_0^*] ds}{\int_s I_y \cdot (\boldsymbol{E} \times \boldsymbol{H}_0^* + \boldsymbol{E}_0^* \times \boldsymbol{H}) ds}, \quad (1)$$

where $\Delta \mathfrak{y} = \mu_0(\mathfrak{y} - 1)$ and $\Delta \epsilon = \epsilon_0(\epsilon_r - 1)$. The Polder permeability tensor[4] is $\mathfrak{y}$, and $\epsilon_0 \epsilon_r$ is the dielectric constant

[2] We must bear in mind here the difference between internal and external fields, especially with regard to configuration 1(a). For a detailed discussion, see R. F. Soohoo, "Theory and Application of Ferrites," Prentice-Hall, Inc., Englewood Cliffs, N. J., pp. 170–172; 1960.

[3] For derivation, see R. F. Soohoo, *op. cit.*, pp. 264–265.

[4] D. Polder, "On the theory of ferromagnetic resonance," *Phil. Mag.*, vol. 40, pp. 99–115; February, 1949.

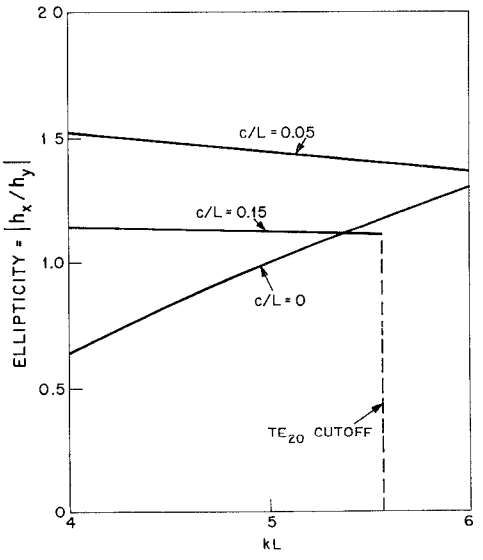

Fig. 4—Ellipticity at the dielectric-air interfaces vs normalized frequency (kL) for a waveguide loaded by a centrally located dielectric slab.

of the ferrite. The cross-sectional areas of the ferrite and guide are Δs and s, respectively. The quantities with and without the zero subscript refer to the electromagnetic fields in the waveguide without and with the ferrite slab, respectively. From (1), we find for the case where the dielectric is centrally located:

$$\frac{\gamma+\gamma_0^*}{j\beta_0}=\frac{A_1\frac{\delta}{2}+A_2\sin k_{ca}(L-c-2\delta)+A_3\sin k_{ca}(L-c)+A_4[\cos k_{ca}(L-c)-\cos k_{ca}(L-c-2\delta)]}{L-c-\frac{1}{k_{ca}}\sin k_{ca}\frac{(L-c)}{2}+\left(\frac{k_{ca}}{k_{cd}}\right)^2\left(c+\frac{\sin k_{cd}c}{k_{cd}}\right)\left[\frac{\cos k_{ca}\frac{(L-c)}{2}}{\sin k_{cd}\frac{c}{2}}\right]}, \quad (2)$$

where

$$A_1=\chi_1+\left(\frac{k_{ca}}{\beta_0}\right)^2\chi_2-\frac{\omega^2\mu_0\epsilon_0(\epsilon_r-1)}{\beta_0^2}$$

$$A_2=\frac{1}{4k_{ca}}\left[\chi_1-\left(\frac{k_{ca}}{\beta_0}\right)^2\chi_2-\frac{\omega^2\mu_0\epsilon_0(\epsilon_r-1)}{\beta_0^2}\right]$$

$$A_3=\frac{1}{4k_{ca}}\left[-\chi_1+\left(\frac{k_{ca}}{\beta_0}\right)^2\chi_2+\frac{\omega^2\mu_0\epsilon_0(\epsilon_r-1)}{\beta_0^2}\right]$$

$$A_4=\frac{K}{2\beta_0},$$

and

$$\chi_1=\frac{\gamma_e^2M_0\left(H_0-\frac{i\alpha\omega}{\gamma_e}\right)}{[\gamma_e^2H_0(H_0+M_0)-\omega^2]-i\alpha\omega\gamma_e(2H_0+M_0)}$$

$$\chi_2=\frac{\gamma_e^2M_0\left(H_0+M_0-\frac{i\alpha\omega}{\gamma_e}\right)}{[\gamma_e^2H_0(H_0+M_0)-\omega^2]-i\alpha\omega\gamma_e(2H_0+M_0)} \quad (3)$$

$$K=\frac{\gamma_eM_0\omega}{[\gamma_e^2H_0(H_0+M_0)-\omega^2]-i\alpha\omega\gamma_e(H_0+M_0)},$$

where H_0 and M_0 are dc magnetic field and magnetization, while γ_e and α are the gyromagnetic ratio and damping constant, respectively.

Noting that $A_{1,2,3}$ all contain terms that involve β_0^2, we conclude that these terms cannot give rise to anisotropic effects. On the other hand, A_4 is inversely proportional to the first power of β_0, thus representing anisotropic effects. Thus, it follows that the differential propagation constant is:

$$\gamma_+-\gamma_-=jK\frac{\cos k_{ca}(L-c)-\cos k_{ca}(L-c-2\delta)}{L-c-\frac{\sin k_{ca}\frac{(L-c)}{2}}{k_{ca}}+\left(\frac{k_{ca}}{k_{cd}}\right)^2\left(c+\frac{\sin k_{cd}c}{k_{cd}}\right)\frac{\cos k_{ca}\frac{(L-c)}{2}}{\cos k_{cd}\frac{c}{2}}}. \quad (4)$$

If $\delta/L\ll 1$, the numerator of (15) may be replaced by $-(K''+jK')k_{ca}2\delta\sin k_{ca}(L-c)$. To appreciate the broadbanding effects of dielectric loading, we have plotted the real part of (4) in Fig. 5 for a ferrite whose $\delta=L/100$, $4\pi M_s=2000$ gauss and $\Delta H=450$ oersteds biased to resonance at a frequency corresponding to $kL=4$. The calculation shows that K'' decreases as kL is increased or decreased from a frequency corresponding to $kL=4$, while the remainder of (4) increases with frequency. Thus, for $kL>4$, it is possible to adjust the values of ϵ_d and c so that $\alpha_+-\alpha_-$ would be less sensitive to frequency over a band of frequencies.

An even more instructive comparison would be to place the ferrite slab at $a=L/4$ of an otherwise empty guide. This location corresponds to the plane of maximum differential propagation in a guide loaded only by a thin ferrite slab, as can be shown from (1). In this case, we find that:

$$\gamma_+-\gamma_-=-j2\pi K\delta/L^2. \quad (5)$$

Thus, the bandwidth of the device is solely determined by the line width of the ferrite. This is in contrast to the dielectric-loaded case whereby (4) indicates that the possibility of compensation exists so that $\gamma_+-\gamma_-$ may vary slowly with frequency. Eq. (5) has also been plotted in Fig. 5 for comparison with the dielectric-loading case. The two curves have been normalized at $kL=4$ by dividing $\alpha_+-\alpha_-$ of the dielectric-loaded case by 144, showing that d_+-d_- is some 150 times larger for the dielectric-loaded case due to the concentration of RF field in the ferrite.

For the case where the ferrite and dielectric configuration is as shown in Fig. 1(b), the boundary-value problem with the dielectric alone is extremely difficult to solve exactly. However, if we assume that the RF field just adjacent to the dielectric is nearly the same as that of the case of a guide loaded by a dielectric slab extending completely across the guide, but that the RF field elsewhere is essentially the same as that of the unloaded

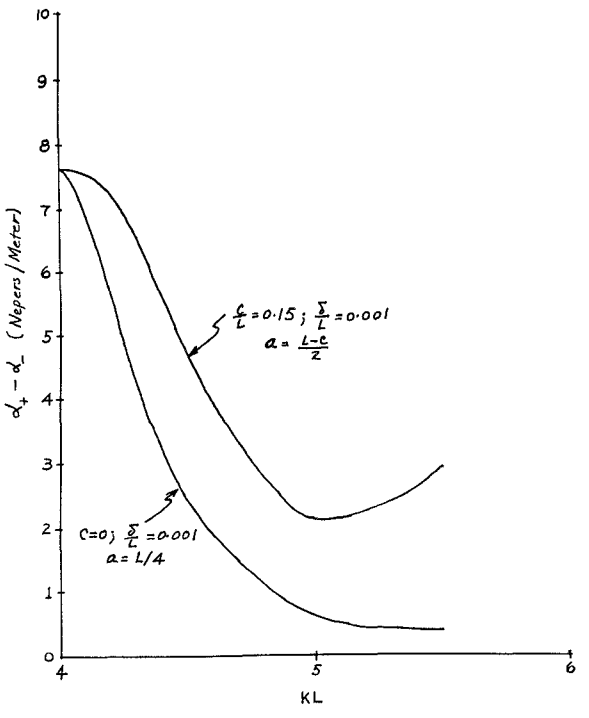

Fig. 5—Differential attenuation vs normalized frequency (kL) for a ferrite isolator loaded and unloaded by a dielectric slab. The normalization factor $(d_+-d_-)_{c=0.15}/(d_+-d_-)_{c=0}$ is equal to 144.

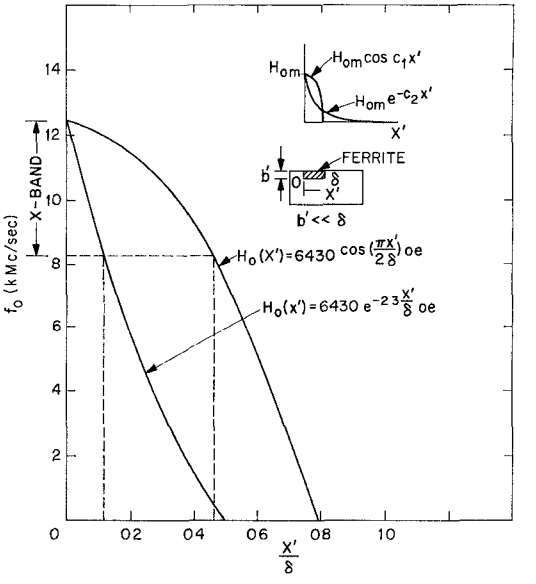

Fig. 6—Resonance frequency of a ferrite sample biased by a tapered dc magnetic field. H_{0m} has been so chosen that $f_0=12.4$ KM_s at $x'=0$, while c_1 and c_2 were so chosen that $H_0(x')=0$ and $H_0(x')=0.1$ H_{0m} at $x'=\delta$ for the cosine and exponential variations, respectively.

case, we can easily show from (1) that:

$$\gamma_+ - \gamma_- = 2jKk_{ca}(\delta/L)(b'/b)\sin k_{ca}2a. \tag{6}$$

Tapered-Field Theory

If the ferrite sample is biased by a spatially varying static magnetic field as shown in Fig. 1(c), we would expect the resonance frequency of different parts of the ferrite to be different. This should give rise to a *distribution of resonance frequencies* and consequently to broadbanding of the device. In Fig. 6, we have plotted the resonance frequency of the ferrite as a function of distance with both a cosine and an exponential variation of the static magnetic field with the distance x'. It is noted that a large portion of the ferrite has its resonance frequency outside x band, and this portion would act essentially as a dielectric, providing $4\pi M_s$ is not so high that low field losses might occur.

The propagation constant of the structure shown in Fig. 1(c) could again be obtained by the perturbation formula (1). For a given static field distribution, we find:

$$\gamma+\gamma_0^* = \frac{j\omega b'}{Lb\left(\frac{f}{f_c}\right)\sqrt{\left(\frac{f}{f_c}\right)^2-1}\sqrt{\frac{\mu_0}{\epsilon_0}}}\left\{\int_a^{a+\delta}[\chi_3(|h_x|^2+|h_y|^2)+jK(h_xh_y^*-h_yh_x^*)]dx - \mu_0\left(\frac{\epsilon_r-1}{\epsilon_r}\right)\left(\frac{f}{f_c}\right)^2\left[\frac{\delta}{2}-\frac{L}{4\pi}\left(\sin\frac{2\pi(a+\delta)}{L}-\sin\frac{2\pi a}{L}\right)\right]\right\} \tag{7}$$

where

$$\chi_3 = \frac{\gamma M_0[\gamma H_0(x)+j\omega\alpha-\gamma M_0]}{[\gamma H_0(x)+j\omega\alpha-\gamma M_0]^2-\omega^2}$$

$$K = \frac{\omega\gamma M_0}{[\gamma H_0(x)+j\omega\alpha-\gamma M_0]^2-\omega^2}. \tag{8}$$

In principle, if $H_0(x)$ is specified, (7) could be integrated to obtain $\gamma+\gamma_0^*$. However, the integration is usually difficult except for the very simple distribution of $H_0(x)$.

As a simple example to illustrate the application of (7) to tapered-field problems, we consider the case where $H_0(x)=H_{0m}(1-c_3(x'/\delta))$. To be definite, we may let $H_{0m}=6430$ *oe*, as is done in Fig. 6, and let $c_3=4430/6430$ so that $H_0(x)=2000=4\pi M_s$ at $x'=\delta$, such that the entire ferrite slab is saturated. From (7) we find the differential propagation:

$$\gamma_+ - \gamma_- = \frac{-j\omega b'\gamma M_0\delta}{Lb\left(\frac{f}{f_c}\right)\sqrt{\frac{\mu_0}{\epsilon_0}}H_{0m}c_3}\left[\log\frac{\frac{\omega}{\gamma_e}+M_0}{\frac{\omega}{\gamma_e}-M_0} - \log\frac{\frac{\omega}{\gamma_e}+H_{0m}-M_0}{\frac{\omega}{\gamma_e}-H_{0m}+M_0}\right]. \tag{9}$$

In the derivation of (9), we have assumed that $K=K'-j0$ for simplicity, so that $\gamma_+-\gamma_-$ will become infinite at resonance. Also, we have assumed that δ is small enough that sin $2\pi x/L$, which occurs in the $h_xh_x^*-h_x^*h_y$ expression, can be replaced by 1 inside the integral, *i.e.*, by setting $x=L/4$ so as to locate the ferrite at the plane of maximum differential propagation.

Further Discussion

From Fig. 3, we observe that the ellipticity for the $c/L=0.15$ case is nearly equal to 1.2, over half of the air-filled region of the waveguide. Thus, a thin slab of ferrite with a width of $x/L\simeq 0.2$ may be placed against the top wall of the waveguide, and adjacent to the dielectric, to obtain good isolation-to-loss ratio or large differential phase shift with low loss over a broad band of frequencies. This configuration has the advantage of higher power-carrying capacity than that of Fig. 1(a). If more isolation or differential phase shift per unit length is desired, two or four ferrite slabs may be placed against the top and/or bottom guide walls on either side of the dielectric slab. In this case, the ferrite slabs on the opposite sides of the dielectric should be oppositely magnetized.

When $\omega<|\gamma_e|(H_a+M_s)$, where H_a is the anisotropy field, low field losses may occur when the ferrite is not saturated. Thus, in the design of tapered-field devices, care should be taken so that the ferrite is saturated at all points, if low field losses would otherwise occur. If the dc magnetic-field configuration is such that this cannot be achieved, it would be best to eliminate the unsaturated portion or to replace that portion by a dielectric of about the same dielectric constant.

Theory of TEM Diode Switching*

ROBERT V. GARVER†, MEMBER, IRE

Summary—**The theory of TEM diode switching is presented for the purpose of understanding and designing TEM microwave diode switches. A few experimental results are reported for the purpose of supporting the theory and demonstrating the exceptional bandwidth possible.**

An analysis is given of the switching action of one and of two or more diodes as well as the biasing of the center conductor of a TEM transmission line over broad-frequency bandwidths without interacting with the RF signal. The use of point-contact germanium, varactor, and gold-bonded germanium diodes for TEM switching is discussed. Some considerations of switching speed and maximum power-handling capacity are given.

A coaxial transmission line switch has been constructed in which two gold-bonded diodes provide 26-db or greater isolation and insertion loss ranging from 1.6 db to less than 1 db from 40 Mc to 4000 Mc. The addition of a bias lead should increase the insertion loss 0.4 db or less over the 100-to-1 bandwidth, the maximum increase being at the upper and lower bounds.

I. Introduction

FOR SOME years a technique for switching microwaves in X-band waveguide with semiconductor diodes has been in use [1]. Attempts to understand this switching action led to a theory of semiconductor diode microwave switching by use of point-contact germanium diodes [2]. Other investigators found a more direct theory for isolation [3] and proved the good possibilities of using varactor diodes [4] and gold-bonded diodes [5] in coaxial transmission lines for switching. This report covers a more thorough investigation of the theory of TEM microwave diode switching and presents some modes of operation heretofore unreported.

When discussing diode switching it is necessary to define certain terms. RF power incident on an ideal attenuating device is either absorbed in or transmitted past the device, with no power reflected. The attenuation α of the device is defined as the ratio in decibels of the incident power to the transmitted power. If the attenuation of the device can be changed from some low value to some high value the device is called a switch. The insertion loss δ is defined as the minimum attenuation, and the isolation η is defined as the maximum attenuation.

When a diode is inserted in series or in shunt in a transmission line, RF power incident on the diode is reflected by, absorbed in, or transmitted past the diode. A diode is different from an attenuating device in that most of the incident RF power not transmitted is reflected rather than absorbed. In fact, in an ideal diode switch, the incident power is either completely reflected or completely transmitted. The definitions of attenuation, insertion loss, and isolation are the same for a diode switch as for an absorption switch.

* Received by the PGMTT, September 20, 1960.
† Diamond Ordnance Fuze Laboratories, Washington 25, D. C.